HHS Public Access

Author manuscript

Nat Chem Biol. Author manuscript; available in PMC 2012 June 01.

Published in final edited form as:

Nat Chem Biol. ; 7(12): 885–887. doi:10.1038/nchembio.687.

N^6-Methyladenosine in Nuclear RNA is a Major Substrate of the Obesity-Associated FTO

Guifang Jia[1,5], **Ye Fu**[1,5], **Xu Zhao**[2,5], **Qing Dai**[1], **Guanqun Zheng**[1], **Ying Yang**[2], **Chengqi Yi**[3], **Tomas Lindahl**[4], **Tao Pan**[3], **Yun-Gui Yang**[2], and **Chuan He**[1,★]

[1]Department of Chemistry and Institute for Biophysical Dynamics, The University of Chicago, 929 East 57th Street, Chicago, Illinois 60637, USA

[2]Genome Structure and Stability Group, Disease Genomics and Personalized Medicine Laboratory, Beijing Institute of Genomics, Chinese Academy of Sciences, No.7 Beitucheng West Road, Chaoyang District, Beijing 100029, PR China

[3]Department of Biochemistry and Molecular Biology, The University of Chicago, Chicago, 929 East 57th Street, Chicago, Illinois 60637, USA

[4]Cancer Research UK London Research Institute, Clare Hall Laboratories, South Mimms, Herts EN6 3LD, UK

Abstract

We report here that FTO (fat mass and obesity-associated protein) exhibits efficient oxidative demethylation activity of abundant *N*^{6}-methyladenosine (m^{6}A) residues in RNA *in vitro*. FTO knockdown with siRNA led to an increased level of m^{6}A in mRNA, whereas overexpression of FTO resulted in a decreased level of m^{6}A in human cells. We further show that FTO partially colocalizes with nuclear speckles, supporting m^{6}A in nuclear RNA as a physiological substrate of FTO.

Obesity has become a serious world-wide public health concern. Fat mass and obesity-associated (FTO) protein has been shown to affect human obesity and energy homeostasis[1–6]. Since the first connection with obesity was made through genome-wide association studies, FTO has become a prominent target of research in the field. However, the physiological substrate and function of FTO remains unknown, which prevents

---

★Correspondence and requests for materials should be addressed to C.H. chuanhe@uchicago.edu.
[5]These authors contributed equally to this work.

Author Contributions

G.J., Y.F., and C.H. conceived the original idea. G.J., Y.F., X.Z., Y.G.Y and C.H. designed the experiments with help from T.P. Biochemistry assays and cellular analysis were performed by G.J., Y.F., and X. Z. with the help of G.Z., C.Y., and Y.Y.; Q.D. carried out the chemical synthesis; T.L. provided advice and the anti-FTO antibody; G.J., Y.F., Y.G.Y. and C.H. wrote the paper.

Competing financial interests

The authors declare no competing financial interests.

molecular level understanding of the mechanism and pathway of the FTO-mediated regulation.

FTO belongs to the non-heme Fe^{II}/α-KG-dependent dioxygenase AlkB family proteins that also includes ABH1 to ABH8[7,8]. Among them, ABH1, ABH2, and ABH3 have been shown to oxidatively demethylate N-methylated DNA/RNA bases[9,10], and ABH8 catalyzes the hydroxylation of hypermodified tRNA wobble uridine[11,12]. FTO has previously been shown to oxidatively demethylate m^3T and m^3U in single-stranded DNA (ssDNA) and single-stranded RNA (ssRNA) *in vitro*[7,13], although the observed activity is exceedingly low compared to those of the other AlkB family proteins[14]. The recent crystal structure of FTO confirms the substrate preference of FTO for single-stranded nucleic acids[15]. Therefore, modified RNAs are plausible substrate candidates for FTO.

Since the physiological substrates of the AlkB family proteins might not be limited to N^1-or N^3-modified purines or pyrimidines, as in the case of ABH8[11,12], we turned our attention to N^6-methyladenosine (m^6A) (Fig. 1a), which is the dominating methylated base in mRNA with a frequency of 3–5 m^6A per mRNA molecule in mammalian cells[16–19]. Although the exact role of m^6A in mRNA is largely unknown, it has been proposed to affect mRNA processing and export from nucleus to cytoplasm[19].

We synthesized ssRNA and ssDNA with site-specifically incorporated m^6A (Supplementary Scheme 1 and Supplementary Fig. 1). After treating an 8-mer ssDNA containing m^6A (1 nmol) with an equal amount of recombinant human FTO (Supplementary Fig. 2) at pH 7.0 at room temperature overnight, we observed a loss of 14 Dalton in mass indicating that a demethylation process had occurred (Supplementary Fig. 3). To further investigate the demethylation activity of FTO towards m^6A in DNA and RNA, we synthesized a series of 15-mer ssDNA and ssRNA containing a central m^6A base. These single-stranded oligonucleotides were treated with 20 mol% of FTO at pH 7.0 at room temperature for 3 h. We then digested the oligonucleotides into nucleosides using nuclease P1 and alkaline phosphatase, and separated the products on a C18 column by HPLC. The HPLC trace profile indicated that m^6A in ssDNA and ssRNA was completely converted to adenosine upon FTO treatment (Fig. 1b,c). We further tested a short m^6A-containing RNA using a known sequence of cellular bovine prolactin (bPRL) mRNA, in which the position of m^6A had been mapped[18,19]. While this short RNA sequence can form a stem loop secondary structure, we still observed 40% of demethylation of m^6A under the same conditions (Fig. 1d). We tested m^6A-containing dsDNA and dsRNA with negligible activity observed under the same reaction conditions (0.2 equivalent of FTO for 3 h). After treatment with one molar equivalent of FTO at 16 °C overnight, we observed a demethylation yield of 40% for dsDNA and 24% for dsRNA, respectively (Supplementary Fig. 4).

To confirm that the observed demethylation requires the oxidative function of FTO, we tested m^6A demethylation using several FTO mutants with active site mutations. Arg316 is a key residue for stabilizing the binding of α-KG. We expressed and purified the FTO R316Q mutant protein (Supplementary Fig. 2), and found that this R316Q mutation abolished 80% of the wild-type activity towards m^6A demethylation *in vitro* (Supplementary Fig. 5). We subsequently constructed and tested two double mutant FTO proteins, H231A/D233A, in

which two iron(II) ligands were mutated, and R316Q/R322Q, in which two α-KG ligands were mutated (Supplementary Fig. 2). Both of these double mutants completely lost m^6A demethylation activity (Supplementary Fig. 5). These results confirmed that FTO catalyzes oxidative demethylation of m^6A in an iron(II)- and α-KG-dependent manner.

We determined detailed reaction kinetics of FTO on a 15-mer m^6A-containing ssRNA at pH 7.0 at 20 °C (Supplementary Fig. 6). The results are summarized in Supplementary Table 1 in comparison to our previously published kinetic data on m^3U in ssRNA at pH 6.0. FTO exhibits a pH-dependent oxidative demethylation activity with the highest activity observed at pH 6.0[13]. Even if we compare the FTO activity towards m^6A at pH 7.0 to that of m^3U at pH 6.0 in ssRNA, we still observe an over 50-fold preference of FTO for m^6A. To further validate this conclusion, we synthesized and tested ssRNA containing m^3U with the same sequence as that used for m^6A at 20 °C (Supplementary Fig. 7). The demethylation activity of FTO towards m^6A is indeed significantly faster than towards m^3U at neutral pH *in vitro*. Under physiological conditions, m^6A is the best substrate discovered so far for FTO.

While m^6A has not been identified in genomic DNA in higher eukaryotes, it is present in easily detectable levels in cellular mRNAs isolated from all higher eukaryotes and viral RNA[16–19]. We explored whether m^6A in mRNA is a physiological substrate of FTO *in vivo*. We transfected HeLa and 293FT cells with *FTO* siRNA (see Supplementary Methods), and western blotting of the total cell lysates from transfected cells showed close to 90% knockdown of FTO 48 h post-transfection (Supplementary Fig. 8a). We then isolated total mRNA from cells treated with control siRNA and *FTO* siRNA using a biotin-poly (dT) probe for separation followed by a rRNA depletion step to ensure depletion of rRNA (see Supplementary Methods and Supplementary Fig. 9). We then digested the total mRNA into nucleosides, and measured the relative amount of m^6A levels by LC-MS/MS. The total contents of m^6A and A were quantified based on a standard curve generated using pure standards, from which the m^6A/A ratio was calculated (see Supplementary Methods and Supplementary Fig. 10). Our results indicated that knockdown of the cellular FTO increased m^6A in mRNA by 23% in HeLa cells and 42% in 293FT cells (Fig. 2a). We also overexpressed wild-type FTO using a mammalian expression vector. Western blotting of the total cell lysates from transfected cells confirmed the overexpression of FTO by 6–8 folds after 24 h (Supplementary Fig. 8b). Total mRNA isolated from HeLa cells overexpressing the wild-type FTO showed a notable decrease of m^6A (~18%) (Fig. 2b).

Since a large portion of m^6A is after G in the consensus sequence (Pu[G>A]m^6AC[A/C/U])[19], we also employed a two-dimensional thin layer chromatography (2D-TLC) method that can detect the m^6A content after G in mRNA (see Supplementary Methods). The results supported the conclusion that the m^6A content in mRNA is affected by the cellular activity of FTO (Supplementary Fig. 11). A dot blot assay using an anti-m^6A antibody was also used to qualitatively monitor the change of m^6A level with the same conclusion obtained (Supplementary Fig. 12). We performed additional western blotting experiments for MT-A70 (AdoMet-binding subunit of mRNA N^6-adenosine-methyltransferase) to confirm that the observed change of the m^6A level was caused by FTO, but not from the potential alteration of the m^6A mRNA methyltransferase expression[20] (Supplementary Fig. 13). Knockdown of FTO in HeLa cells led to a decrease of MT-A70 expression of around 15%,

and overexpression of FTO led to an increase of MT-A70 expression of about 15%. Furthermore, knockdown of ABH3 in HeLa cells did not noticeably affect the total level of m^6A in mRNA as a negative control (Supplementary Fig. 14). We conclude that the increase of the m^6A level in the FTO knockdown sample is not due to an increased level of methyltransferase, but is a result of the depletion of cellular FTO.

Lastly, indirect immunofluorescence analysis was performed to visualize the localization of the FTO protein in mammalian cells. FTO is known to be entirely localized to cell nuclei[7]. We observed that the cellular FTO protein is present in a dot-like manner in nucleoplasm, and partially colocalizes with splicing or splicing-related speckle factors SART1(U4/U6.U5 tri-snRNP-associated protein 1) and SC35 (serine/arginine-rich splicing factor 2), and RNA polymerase II phosphorylated at Ser2 (Pol II-S2P) (Fig. 3a and Supplementary Fig. 15a,b), but does not colocalize with telomere marker TRF1, replication site PCNA, Cajal body marker Coilin, cleavage body marker CstF64, or P-body marker DCP1A (Supplementary Fig. 16a and 17). To investigate whether FTO is related to mRNA processing, we performed the same immunostaining experiment upon inhibition of Pol II-S2P transcription with actinomycin D (ActD). Quantitative foci analysis showed that the FTO foci number per cell was significantly decreased from 43±7 (−ActD) to 22 ± 5 (+ActD) with *P*-value less than 0.0001, similar to that observed for Pol–II S2P from 90 ± 12 (−ActD) to 24 ± 5 (+ActD), but not SC35[21] (Fig. 3b), upon transcription inhibition (Supplementary Fig. 18). Intriguingly, the decreased FTO nucleoplasm foci became more concentrated into discrete speckle foci after transcription inhibition by ActD (Fig. 3a and Supplementary Fig. 15a), resembling that of Pol II-S2P[21] (Supplementary Fig. 15a). Moreover, the transcription inhibition induced a more pronounced colocalization of FTO with both SC35 and Pol II-S2P (Fig. 3a and Supplementary Fig. 15a). Splicing speckles are major nuclear domains enriched for components of the splicing machinery such as SC35, polyA+ RNA, and numerous mRNA metabolic factors[21–24]; genes associated with splicing speckles have been shown to function in spliceosome assembly or post-transcriptional splicing of pre-mRNAs[23,24]. Knockdown of FTO does not affect the assembly of spliceosome (Supplementary Fig. 16b,c); however, FTO shows a distribution pattern in nuclear speckles similar to other splicing factors. FTO may be recruited to the speckles by its interacting partners in the assembled nuclear speckles. In conclusion, the partial colocalization of FTO with nuclear speckles further supports the concept that m^6A in nuclear RNA is a substrate of FTO, and the enzymatic alteration may be linked to processing of recently transcribed mRNA.

In summary, we show that FTO efficiently demethylates m^6A at neutral pH *in vitro*, and the level of m^6A in cellular mRNA is affected by the oxidation activity of FTO *in vivo*. FTO partially localizes with nuclear speckles. The pronounced concentration of FTO in speckles upon Pol II-S2P transcription inhibition suggests a dynamic interaction of FTO with the nuclear speckles. In fact, MT-A70, a critical subunit of m^6A-methyltransferase that introduces m^6A into mRNA, has also been shown to localize in nuclear speckles, and probably associates with nuclear pre-mRNA splicing components[20]. All these observations indicate that m^6A in nuclear RNA is the physiological substrate of FTO, and that the function of FTO likely affects the processing of pre-mRNA and/or other nuclear RNAs.

Despite past research on m^6A in mRNA, the biological function of this ubiquitous post-transcriptional modification remains unclear, particularly in mRNA from higher eukaryotes. Our cellular data suggest that a portion or subclass of m^6A in mRNAs appeared to be affected by the activity of FTO *in vivo*. How the sequence and methylation status of m^6A in mRNA affect the output of RNA still requires detailed investigation; the fact that the function of the major obesity factor FTO is to demethylate m^6A in mRNA clearly indicates a novel, reversible regulatory mechanism present in mammalian cells. Methylation of DNA and histones contributes largely to epigenetic regulation in mammalian cells. The discovery of the FTO-mediated oxidative demethylation of m^6A in nuclear RNA may initiate further investigations on biological regulation based on reversible chemical modification of RNA[25].

Supplementary Material

Refer to Web version on PubMed Central for supplementary material.

Acknowledgments

This work was supported by the U.S. National Institute of Health (GM071440 to C.H.), an NIH EUREKA award (GM088599 to C.H. and T.P.), and the CAS “100-talents” Professor Program to Y.G.Y. Q.D. was supported by the Chicago Biomedical Consortium (CBC). X.Z. and Y.Y. supported by Graduate Student Program of Beijing Institute of Genomics, Chinese Academy of Sciences (CAS). T.L. supported by the CAS Senior Foreign Research Fellow Award (2009S2-1). We thank CBC/UIC RRC Proteomics and Informatics Services Facility for performing the LC-MS/MS analysis, L.A. Godley for the suggestion, and P. Jin for providing the pcDNA3-FTO plasmid. We thank Sarah Frank Reichard, M.A. for editing the manuscript.

References

1. Laura LJ, et al. Science. 2007; 316:1341–1345. [PubMed: 17463248]
2. Frayling TM, et al. Science. 2007; 316:889–894. [PubMed: 17434869]
3. Dina C, et al. Nat Genet. 2007; 39:724–726. [PubMed: 17496892]
4. Thorleifsson G, et al. Nat Genet. 2009; 41:18–24. [PubMed: 19079260]
5. Fischer J, et al. Nature. 2009; 458:894–898. [PubMed: 19234441]
6. Church C, et al. Nat Genet. 2010; 42:1086–1092. [PubMed: 21076408]
7. Gerken T, et al. Science. 2007; 318:1469–1472. [PubMed: 17991826]
8. Kurowski MA, Bhagwat AS, Papaj G, Bujnicki JM. BMC Genomics. 2003; 4:48. [PubMed: 14667252]
9. Westbye MP, et al. J Biol Chem. 2008; 283:25046–25056. [PubMed: 18603530]
10. Aas PA, et al. Nature. 2003; 421:859–863. [PubMed: 12594517]
11. Fu Y, et al. Angew Chem Int Ed Engl. 2010; 49:8885–8888. [PubMed: 20583019]
12. van den Born E, et al. Nat Commun. 2011; 2:172. [PubMed: 21285950]
13. Jia G, et al. FEBS Lett. 2008; 582:3313–3319. [PubMed: 18775698]
14. Lee DH, et al. J Biol Chem. 2005; 280:39448–39459. [PubMed: 16174769]
15. Han Z, et al. Nature. 2010; 464:1205–1209. [PubMed: 20376003]
16. Wei CM, Gershowitz A, Moss B. Cell. 1975; 4:379–386. [PubMed: 164293]
17. Narayan P, Rottman FM. Science. 1988; 242:1159–1162. [PubMed: 3187541]
18. Horowitz S, Horowitz A, Nilsen TW, Munns TW, Rottman FM. Proc Natl Acad Sci USA. 1984; 81:5667–5671. [PubMed: 6592581]
19. Harper JE, Miceli SM, Roberts RJ, Manley JL. Nucleic Acids Res. 1990; 18:5735–5741. [PubMed: 2216767]
20. Bokar JA, Shambaugh ME, Polayes D, Matera AG, Rottman FM. RNA. 1997; 3:1233–1247. [PubMed: 9409616]

21. Xie SQ, et al. Mol Biol Cell. 2006; 17:1723–1733. [PubMed: 16467386]
22. Hall LL, et al. Anat Rec A Discov Mol Cell Evol Biol. 2006; 288:664–675. [PubMed: 16761280]
23. Lawrence JB, Clemson CM. J Cell Biol. 2008; 182:1035–1038. [PubMed: 18809719]
24. Lamond AI, Spector DL. Nat Rev Mol Cell Biol. 2003; 4:605–612. [PubMed: 12923522]
25. He C. Nat Chem Biol. 2010; 6:863–865. [PubMed: 21079590]

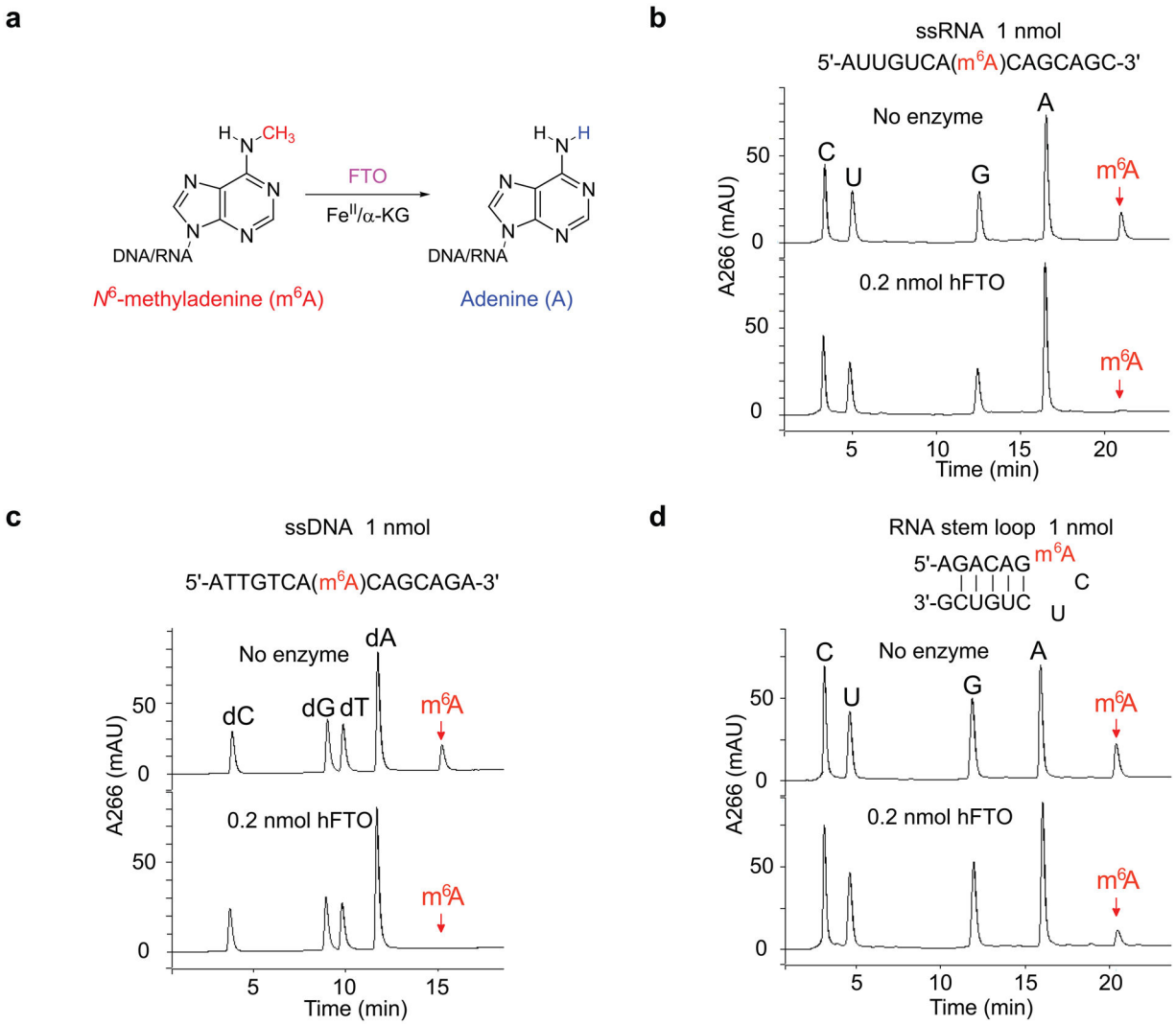

Figure 1. Oxidative demethylation of m^{6}A in nucleic acids by FTO

(**a**) Proposed oxidative demethylation of m^{6}A to A in DNA and RNA by FTO in the presence of iron(II) and α-KG. (**b**, **c**) As shown by HPLC profiles of digested substrates, 20 mol% of FTO can completely demethylate m^{6}A in ssRNA and ssDNA in 3 h at room temperature at neutral pH. (**d**) About 40% demethylation of m^{6}A in a RNA stem loop could be observed under the same reaction conditions.

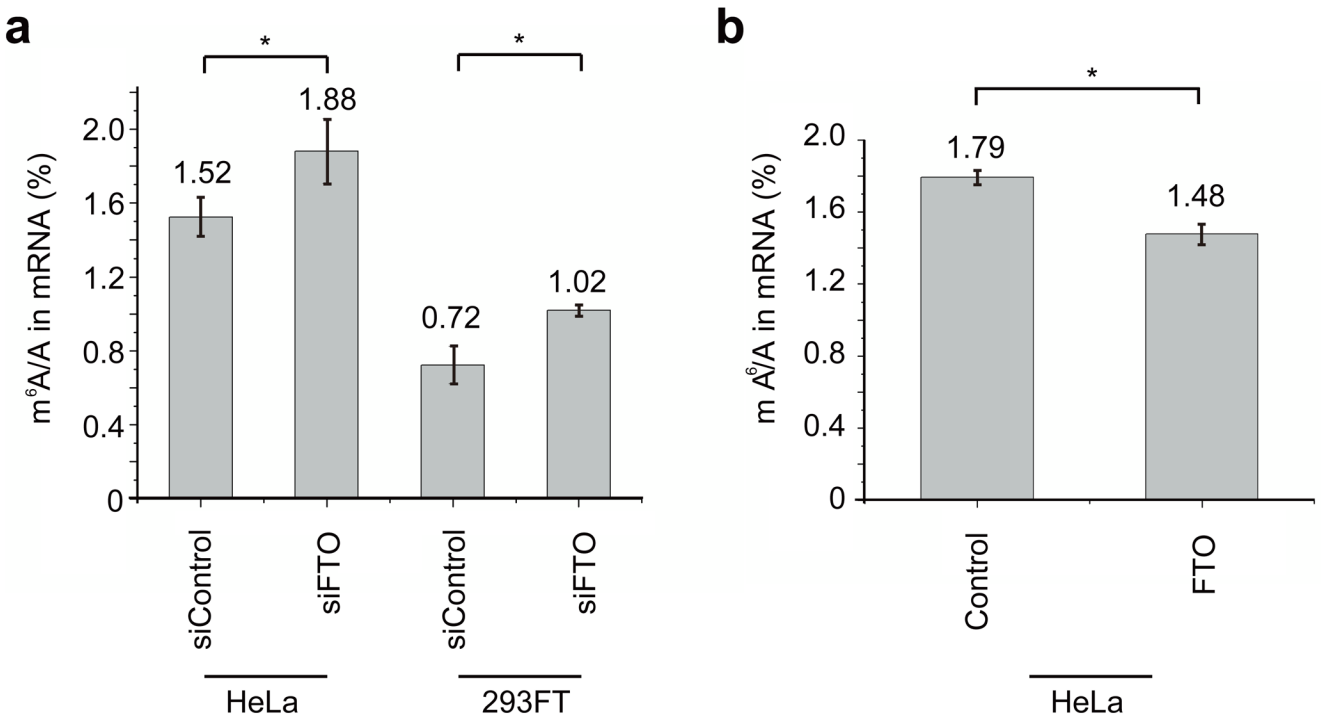

Figure 2. FTO regulates m^{6}A content in mRNA in a FTO-activity dependent manner

(**a**) Quantification of the m^{6}A/A ratio in mRNA by LC-MS/MS. Significant increase of the m^{6}A level was observed in both *FTO* siRNA-treated HeLa and 293FT cells after 48 h. *, *P*-value < 0.05, Student's t-test; means ± s.e.m. for n = 8 experiments. (**b**) The m^{6}A/A ratio of mRNA samples isolated from cells with overexpressed FTO. The overexpression of wild-type FTO decreased the m^{6}A content significantly. * *P*-value < 0.05, Student's t-test; means ± s.e.m. for n = 8 experiments.

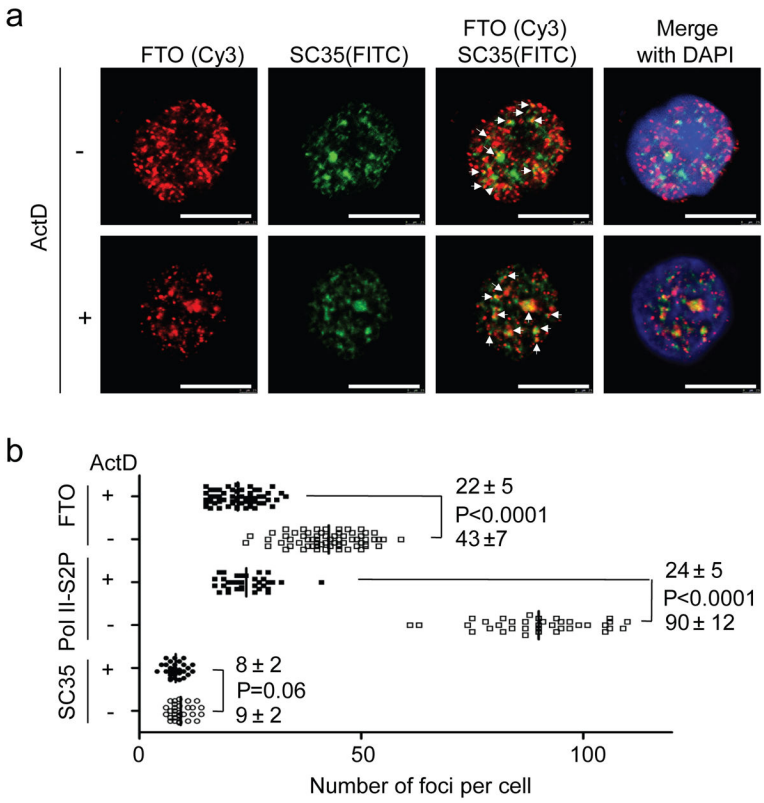

Figure 3. Indirect immunofluorescence analysis of endogenous FTO shows FTO partially colocalizes with nuclear speckles

(**a**) HeLa cells were co-stained with antibodies against FTO and speckle marker SC35 in the presence or absence of transcription inhibitor actinomycin D (ActD). Yellow dots indicated by white arrows correspond to the colocalized spots of FTO (Red) with SC35 (Green) (N = 150). Upon transcription inhibition, the FTO loci number decreased in the nucleoplasm, but its speckle distribution became more pronounced. (**b**) Quantitative foci analysis of SC35, Pol II-S2P, and FTO with (+), or without (−) ActD treatment. 30, 37 and 67 cells were randomly selected for foci analysis of SC35, Pol II-S2P, and FTO, respectively. The t-test using two-way ANOVA in Grouped Analyses of Prism5 software was applied for statistical analysis. *P*-value less than 0.01 was considered a significant difference. The mean numbers of foci per cell for each sample with and without ActD treatment were shown above, and below the corresponding *P*-value, respectively. The foci number of Pol II-S2P and FTO decreased significantly upon transcription inhibition.